





Cite this: *RSC Sustainability*, 2025, 3, 5601

Mechanochemical synthesis of phthalimides from terpenes *via* tandem Diels-Alder cycloaddition and iodine-mediated aromatization

Jhully Anne Barros Carvalho Ribeiro, ^a Renan Rodini Mattioli, ^a
Duncan L. Browne ^b and Julio C. Pastre ^{*a}

A solvent-minimized, two-step mechanochemical protocol has been developed for the synthesis of terpene-derived phthalimides *via* sequential Diels-Alder cycloaddition and iodine-mediated aromatization at room temperature. Efficient conversion of isoprene and maleimides by ball-milling yields adducts in up to 86% yield, followed by *in situ* aromatization using iodine and 1,1,3,3-tetramethylguanidine to furnish phthalimides in up to 82% yield. The process tolerates a range of functional groups and is sensitive to steric hindrance around the diene and dienophile. This method circumvents conventional thermal protocols, offering a scalable and operationally simple route to value-added aromatics from renewable feedstocks under ambient conditions.

Received 27th June 2025
Accepted 13th October 2025

DOI: 10.1039/d5su00509d

rsc.li/rscsus

Sustainability spotlight

The development of environmentally responsible methods for producing value-added chemicals from renewable resources is essential for advancing sustainable industry and consumption. In this study, a mild, scalable, and solvent-free mechanochemical protocol was developed for the synthesis of terpene-derived phthalimides, avoiding toxic reagents, excess energy consumption, and solvent waste. This strategy replaces traditional multi-step thermal processes with a one-pot tandem reaction under ambient conditions, showcasing the power of enabling technologies in green chemistry. The methodology maximises atom economy, minimises environmental impact, and valorises abundant biomass. These achievements directly support UN Sustainable Development Goals 9 (Industry, Innovation and Infrastructure) and 12 (Responsible Consumption and Production), demonstrating a significant step forward in the design of sustainable chemical processes.

Introduction

The design of modern chemical processes is increasingly guided by the principles of green chemistry, which emphasize atom economy, solvent minimization, energy efficiency, and the reduction of resource consumption. In this scenario, modern synthetic chemistry faces the challenge of developing methodologies that minimize human health and environmental impact without compromising process efficiency, selectivity or scalability, requiring significant experimental effort and creativity.¹⁻³

In response to social and environmental demands, new enabling technologies have been integrated into modern chemistry.⁴ Among them, mechanochemistry has emerged as a strategic platform for organic synthesis, offering access to new reactivity modes and solvent-minimized protocols under mild conditions.^{5,6} Recent advances have demonstrated that

mechanically induced reactions can unlock synthetic routes that are challenging or even inaccessible *via* solution-based methods. Furthermore, these protocols often operate under solvent-free, atmospheric and energy-efficient conditions, providing simpler and greener alternatives to conventional approaches.⁷⁻¹²

Mechanochemistry can also be implemented on larger scales, either through the use of very large milling devices or by alternative approaches such as resonant acoustic mixing (RAM) and twin-screw extrusion (TSE), which allow scale-up without substantially increasing the equipment footprint,^{13,14} an important consideration for the treatment of renewable raw materials, such as chitin and microcrystalline cellulose.^{15,16} Furthermore, mechanochemical processes can be designed as one-pot or cascade processes, minimizing workup and tedious purification steps.^{17,18} As a result, mechanochemistry provides simpler and greener alternatives to conventional approaches, with significant reductions in solvent use, reaction time, and waste generation, as demonstrated by the solvent-free dehydrogenation of γ -terpinene in a ball mill, which achieved quantitative yields in just 5 minutes, aligning with key principles of process sustainability.^{15,19}

^aInstitute of Chemistry, State University of Campinas (UNICAMP), 13083-970, Campinas, SP, Brazil. E-mail: jpastre@unicamp.br

^bDepartment of Pharmaceutical and Biological Chemistry, School of Pharmacy, University College London (UCL), 29-39 Brunswick Square, WC1N 1AX London, UK. E-mail: duncan.browne@ucl.ac.uk



Similar to furans, terpenes also occupy a significant global market and drive innovations in platform technologies, such as in cosmetics, biofuels, rubber, food, fragrances and drugs.²⁰ The term terpene originated from turpentine (*Balsamum terbinthinae*), a resin obtained from pine trees, and is also present in coniferous wood, citrus fruits, eucalyptus and several other plants. The abundance and wide availability of terpenes in natural sources make the optimization of extraction methods a relevant field of study. The diversity of these sources requires considering variables such as harvest location and time, in addition to specific pretreatments, solvents, and extraction techniques, to ensure efficient recovery and the preservation of the compounds' chemical profile.^{21,22}

A common characteristic of many terpenes is the presence of an isoprene structure (2-methyl-1,4-butadiene) as a basic unit in the carbon skeleton. These backbones are classified according to the number of isoprene units following the $(C_5H_8)_n$ formula. In the realm of biomass conversion, terpenes have great potential for chemical valorization due to their suitable structural and reactivity characteristics.^{21,23} Although terpenes have long been employed as cost-effective and suitably functionalised starting materials in organic synthesis, their full potential for chemical valorisation remains underexplored, particularly in the context of generating novel chemical entities. For instance, isoprene is widely used as a starting material in the production of terephthalic acid obtained by the oxidation of the



Fig. 1 Terpenes and terpenoids as powerful starting materials for chemical valorization towards aromatics.



p-xylene intermediate (Fig. 1a).²⁴ Terephthalic acid is one of the main precursors for the production of polyester polymers, such as polyethylene terephthalate (PET), which is extensively applied in packaging and synthetic fibers.^{24–28}

Although these representative approaches demonstrate the use of isoprene as a bio-based raw material for the synthesis of industrially relevant aromatic compounds, there is still a dependence on severe reaction conditions (high temperatures and pressures) and metal usage over multiple stages. In 2016, iodine was used as a key promoter for the aromatization of a wide variety of terpenes and terpenoids under thermal conditions *via* carbocation pathways (Fig. 1b).²⁹ Based on previous studies, the authors proposed that other dienes could be converted to their aromatic analogues through rearrangements and migrations, thus enabling the aromatization of quaternary centers. However, despite being metal-free, these protocols still usually require high temperatures and long reaction times.

Our research group has previously explored DA reactions involving terpenes and maleic anhydride in the solution-phase employing continuous flow technology to achieve high-yielding DA adducts (Fig. 1c), which are potentially useful for new green polymers.³⁰ Building on this precedent, we sought to develop a solvent-minimized room-temperature protocol for the direct conversion of terpenes into aromatics under mechanochemical conditions.

Results and discussion

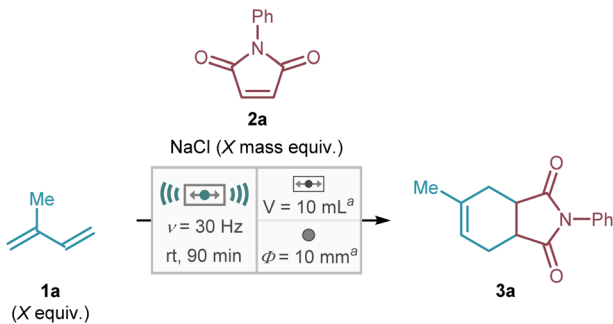
DA reaction investigations

To lay the groundwork and provide a basis for comparison with the solid-state synthesis, we started our study with the DA reaction using isoprene and maleimide at equimolar stoichiometry in diethyl ether (0.2 M) at room temperature for 18 hours.³¹ Since this was not successful, we decided to investigate the stoichiometry of isoprene, temperature, and solvent. Best results were then obtained using 2.0 equiv. of isoprene in ethanol (0.2 M) at 90 °C for 5 hours affording 78% and 84% yield for maleimide and *N*-phenylmaleimide, respectively. At this point, we defined isoprene and *N*-phenylmaleimide as model starting materials for subsequent investigations.

Based on preliminary results, we decided to evaluate the DA reaction under mechanochemical conditions. Our initial tests involved the screening of milling jar volume, milling ball diameter, isoprene equiv., sodium chloride mass equiv. and time (see Table S2 for the full range of conditions tested).

First reactions were performed at room temperature for 90 minutes using a stoichiometric amount of isoprene (**1a**) and *N*-phenylmaleimide (**2a**). In the absence of sodium chloride, the DA adduct was obtained in a very low yield of 6% (Table 1, entry 1). The addition of 0.5 mass equiv. of sodium chloride as the grinding auxiliary increased the yield to 36% (Table 1, entry 2). Increasing sodium chloride to 2.5 mass equivalents improved the yield to 60%, highlighting its key role as a grinding auxiliary (Table 1, entry 3). Conversely, the yield resulted in a significant drop to 45% when 5.0 mass equiv. was used (Table 1, entry 4). Then, increasing isoprene equiv. from 1.0 to 2.0 with 2.5 mass

Table 1 Mechanical DA between isoprene (**1a**) and *N*-phenylmaleimide (**2a**)



Entry ^a	Isoprene (equiv.)	NaCl (mass equiv.)	Yield ^b (%)
1	1.0	—	6
2	1.0	0.5	36
3	1.0	2.5	60
4	1.0	5.0	45
5	2.0	2.5	60
6	2.0	5.0	69
7	3.0	5.0	98 (86) ^c
8 ^d	3.0	5.0	98 (86) ^c

^a Stainless steel materials. ^b Determined by ¹H NMR analysis using mesitylene as the internal standard and deuterated chloroform at 0.1 M concentration. ^c Isolated yield. ^d 25 mL volume milling jar and 15 mm diameter milling ball.

equiv. of sodium chloride led to no enhancement in yield. Probably, doubling isoprene amount can negatively interfere with the powder formation in the grinding process (Table 1, entry 5). However, when sodium chloride is raised to 5.0 mass equiv., the yield slightly increases to 69% (Table 1, entry 6). When isoprene is raised to 3.0 equiv., DA adduct **3a** is ultimately produced in 98% yield followed by a subsequent purification to 86% yield (Table 1, entry 7). We propose that the optimal DA grinding process may be achieved when sodium chloride is employed as the grinding auxiliary in a mass equiv. amount approximately equal to twice that of isoprene. In fact, the presence of a solid auxiliary is crucial for most grinding processes involving liquid reactants, enabling the reaction to proceed in a powdered state and optimizing mass and energy transfer.⁶ On the other hand, the high volatility of isoprene suggests that an excess would be necessary in the reaction.

The successful synthesis of DA adduct **3a** within satisfactory conversion and yield drove our efforts to further develop a sustainable, safe, and one-pot phthalimide synthesis process. As the aromatization reaction requires more reactants, we judged it necessary to transfer the reaction to a 25 mL milling jar, ensuring that the grinding process would not be compromised. In terms of milling jar volume, the degree of filling – including the space occupied by the milling ball, reactants and grinding auxiliaries – plays a crucial role in energy transfer of the reaction. Considering this, we opt to evaluate the performance of the DA reaction in the 25 mL volume milling jar using



a 15 mm diameter milling ball. Fortunately, the adjustments resulted in unchanged conversion and yield values for the synthesis of DA adduct **3a** (Table 1, entry 8).

Aromatization investigations

Motivated by promising results obtained in the DA reaction by milling, we turned our attention to solution-phase experiments in order to achieve phthalimides through the aromatization of DA adducts. Initially, we performed a screening of conditions as indicated in Table S3 available in the SI. Different reaction conditions were evaluated, including the use of oxidants such as Pd/C³² and DDQ, the combination of H-Y zeolite and Pd/C,³³ acidic conditions with Amberlyst-15,³⁴ and more severe conditions employing elemental sulfur.³⁵ The final crude reaction mixtures were analyzed by gas chromatography-mass spectrometry (GC-MS), and only those in which the desired product was identified were further investigated. However, no condition led to yields or selectivities that justified the continuation of solution-based studies.

Afterwards, we decided to adopt a methodology proposed by Domingos *et al.*²⁹ to convert DA adduct **3a** into the desirable phthalimide. This methodology describes the aromatization of terpenes in the presence of I₂ under solution-phase conditions depicted in Fig. 1b. Surprisingly, when we applied the reported conditions to DA adduct **3a**, we did not detect the formation of the expected phthalimide. Consequently, we decided to investigate harsh conditions in the solution-phase. Initially, we substituted toluene with dimethyl sulfoxide to enable higher temperatures and evaluated acidic, basic and oxidant reaction conditions (see Tables S4–S6 for the full range of conditions tested).

The most satisfactory outcome was obtained by conducting the reaction in two separate steps. First, DA adduct **3a** is combined with 2.0 equiv. of iodine in dimethyl sulfoxide for 30 minutes at 140 °C, and then 2.0 equiv. of DBU is added and reacted for additional 30 minutes at the same temperature, yielding 65% after two steps (¹H NMR measurement using an internal standard).

In our efforts to identify the optimal conditions, we systematically examined the impact of temperature, solvent, solution concentration and addition sequence of reactants on the reaction. In most cases, we observed a rapid consumption of DA adduct **3a** accompanied by low yields of the desired phthalimide (see Table S7 in the SI). In the absence of base, iodine could mediate the aromatization step yielding 40% of the desired phthalimide with full conversion of DA adduct **3a**.

Based on these early findings and TLC analysis, we propose that the base acts as an additive, reducing the formation of unwanted side products in solution. Consequently, we chose to investigate alternative bases, including 1,4-diazabicyclo[2.2.2]octane (DABCO) and 1,1,3,3-tetramethylguanidine (TMG), but unfortunately we did not observe any improvement despite the complete consumption of the DA adduct **3a**.

After verifying the feasibility of solution-phase aromatization of DA adduct **3a**, attention was then directed towards the aromatization step under mechanochemical conditions.

Table 2 Mechanical aromatization of DA adduct **3a**



Entry ^a	I ₂ (equiv.)	Base (equiv.)	Jar (mL)	Ball (mm)	Yield ^b (%)
1	2.0	DBU (3.0)	10	10	33
2	2.0	DBU (5.0)	10	10	33
3	2.0	DBU (5.0)	25	15	45
4	3.0	DBU (5.0)	25	15	54
5	3.0	TMG (3.0)	25	15	66
6	3.0	TMG (4.0)	25	15	75
7	3.0	TMG (5.0)	25	15	93 (82) ^c

^a Stainless steel materials. ^b Determined by ¹H NMR analysis using mesitylene as the internal standard and deuterated chloroform at 0.1 M concentration. ^c Isolated yield.

Preliminary experiments showed that the reaction using 2.0 equiv. of iodine, 3.0 equiv. of DBU and 2.5 mass equiv. of sodium chloride at room temperature for 90 minutes afforded phthalimide **4a** in 33% yield (Table 2, entry 1). Our subsequent investigations involved the screening of jar volume, ball diameter, iodine equiv., base equiv., sodium chloride mass equiv. and time (see Table S8 for the full range of conditions tested). We found that increasing the DBU amount to 5.0 equiv. had no impact on the yield (Table 2, entry 2).

We believe that the aromatization of the DA **3a** adduct occurs by an iodine-mediated mechanism. In the presence of bases such as DBU and TMG, the alkene reacts readily with molecular iodine, forming the iodonium ion. Subsequently, the vicinal diiodide is formed through a replacement mechanism with the iodide anion. In the subsequent step, the base abstracts a proton, leading to the formation of a new π bond and the release of the iodide anion. Subsequent iodide elimination led to another new π bond formation, and then spontaneous aromatization took place. However, it should be noted that – alternatively and/or simultaneously – alpha iodination of the carbonyl followed by further elimination of hydrogen iodide can also proceed. The formation of the strong acid HI could account for the low yield obtained without bases due to acid-catalyzed polymerization of the olefins.

Consistent with our expectations, the use of a 25 mL volume milling jar and 15 mm diameter milling ball led to a modest increase in yield to 45% (Table 2, entry 3). Larger jar volume and ball mass improve energy transfer, increasing yield from 33% to 45% at identical milling frequency. Furthermore, the increase in yield observed in this second system may also be associated with the better energy kinetics involved. Given the mass-dependent nature of kinetic energy, the 15 mm milling ball (13.87 g of mass) is expected to transfer over three times the kinetic energy of the 10 mm milling ball (4.11 g of mass) at an equivalent frequency.



Increasing iodine equiv. to 3.0, the yield improved to 54% (Table 2, entry 4). At this point, we observed that the aromatization step in the solid-phase seemed to be more selective when compared to the solution-phase. We thus selected bases that

showed high conversion rates but low yields in solution-phase reactions to investigate their reactivity in milling. Using TMG as the base, the yield was improved to 66% using 3.0 equiv. of TMG (Table 2, entry 5). Gratifyingly, increasing gradually TMG



Scheme 1 Optimized one-pot tandem protocol for the production of phthalimides 4a–4s. ^aStainless steel materials. *Non-terpene DMBD was used.



equiv. to 4.0 and 5.0 afforded phthalimide **4a** in 75% and 93% yield, respectively (Table 2, entries 6 and 7). More details can be found in the SI along with solution-phase comparisons. After achieving optimal conditions for the iodine-mediated aromatization of DA adduct **3a** to phthalimide **4a** through milling, we expanded our research to the development of a one-pot tandem protocol (Scheme 1). Fortunately, we were able to successfully integrate the two steps by adjusting the mass equivalent of sodium chloride, as both stages were already optimized under identical grinding conditions (frequency, jar volume, and ball diameter). Thus, we performed the DA step with 5.0 mass equiv. of sodium chloride and added only the difference to complete 2.5 mass equiv. in the further aromatization step.

After integration of mechanical DA and iodine-mediated aromatization, we decided to explore a short scope using different terpenes and maleimides. The optimized conditions were successfully applied to three different terpenes and *N*-substituted maleimides, obtaining a library of nineteen phthalimides yielding around 65% on average for both steps (Scheme 1).

Remarkably, structural variations in both diene and dienophile starting materials led to significant changes in yield. A maximum yield of 82% was achieved when the reaction was conducted with isoprene and *N*-phenylmaleimide (Scheme 1, **4a**). The change of isoprene to myrcene caused a dramatic drop in yield to 33% for phthalimide **4b**. Surprisingly, when ocimene is reacted with *N*-phenylmaleimide, phthalimide **4c** is obtained in 80% yield. Bearing a bulkier substituent, DA adduct **3b** differs from **3a** and **3c** analogues, which have a methyl group attached to the sp^2 carbon. According to the proposed mechanism, where aromatization is initiated by iodine addition to the double bond, the lower yield of **4b** can be attributed to steric hindrance caused by the bulky group in **3b**. This steric effect may impede iodine's approach to the reaction site, thereby compromising the efficiency of the initial step.

The observation of a favorable methyl effect during aromatization led us to select isoprene for further exploration in the scope. Bulky groups attached to the maleimide, such as 1-naphthyl and 1-adamantyl, resulted in significantly poorer results (10% for phthalimide **4k** and 27% for phthalimide **4s**). Also, when non-substituted maleimide is used, a very low yield was observed (14% for phthalimide **4d**). In an effort to understand the mesomeric effect, we assessed the impact of diverse functional groups at the *para* position of *N*-phenyl substituted maleimides. No clear trend was observed with *para*-substituted maleimides, indicating minimal mesomeric influence on yield.

The disparate yields of phthalimides **4b**, **4d** and **4s** prompted us to investigate whether the low yields were a consequence of the integrated process or a specific step. For phthalimide **4b**, the DA step presents a yield of around 69%, while the aromatization step yields 50% from the isolated DA adduct. Unfortunately, no improvement was observed even after using BHT-stabilized β -myrcene, showing that probably the yield is highly limited by steric hindrance from the substrate. For phthalimide **4d**, we observed 57% and 42% yield for the DA step, with and without Lewis acid ($AlCl_3$, 20 mol%), respectively. On the other hand, the aromatization step separately led to 75% yield, indicating that the integrated process possibly diminishes the production of phthalimide.

Our milling protocol for the preparation of phthalimides harnesses renewable feedstocks (terpenes) at room temperature under solvent-minimized conditions. To further strengthen its green credentials, we assessed our protocol using sustainability metrics. Aromatization was identified as the key step, and we therefore selected it for comparison. Two plausible benchmarks were considered, the first contrasting our milling methodology with the solution-phase approach, for which we had developed and optimized the synthesis of phthalimide **4a** (Table 3, entries 1 and 2). The latter comparison involved our milling methodology and the study by Domingo *et al.*,²⁹ which served as inspiration for optimizing the mechanochemical synthesis of phthalimide **4a**. For this second comparison, we chose the starting material methyl hydroabietate, which was selected as the closest example to a convenient comparison. However, it was challenging to identify alternative methodologies from other authors that preserved the same reaction characteristics, including the starting material, aromatization reagents, and final product.

In Table 3, we selected the parameters yield, reaction mass efficiency and process mass intensity, which in turn was separated into process mass intensity of reaction, process mass intensity of work-up and total process mass intensity. Process mass intensity of purification was not included in total process mass intensity due to lack of information.

From the comparison between our methodologies, the milling condition yield (process 1) is not only slightly higher, but also affords a RME that is roughly 4 times higher than in the solution-phase protocol (process 2). Furthermore, all PMI instances are at least threefold lower, highlighting the significant technological advantage achieved in the aromatization of DA adduct **3a** to phthalimide **4a**.

When we compare our milling aromatization of DA adduct **3a** to phthalimide **4a** (process 1) with methyl hydroabietate aromatization in the solution-phase (process 3), we note that in

Table 3 Sustainable metrics comparison between milling (1) and solution-phase (2 and 3) methods of iodine-mediated aromatization^a

Process	Yield (%)	RME (%)	PMI _R (g g ⁻¹)	PMI _{WU} (g g ⁻¹)	PMI _T (g g ⁻¹)
1	89	5.6	17.8	888.0	905.8
2	72	1.4	71.5	3292.6	3364.1
3	84	6.5	15.3	3632.9*	3648.2*

^a RME: Reaction mass efficiency. PMI_R: Process mass intensity of reaction. PMI_{WU}: Process mass intensity of work-up. PMI_T: Total process mass intensity. *Without considering NaSO₄ used in work-up due to lack of information.



terms of RME process 3 takes slightly the lead because of less use of reactants compared to process 1 (6.5% *versus* 5.6%). Finally, the most precise metric to measure the resource utilization is obtained in process mass intensity. It is worth noting that process 3 has 4-fold higher PMI_T than process 1 to afford the analogue product in similar comparable yield (3648.2 g g⁻¹ *versus* 905.8 g g⁻¹). Furthermore, the major contribution to PMI_T in process 3 is derived from solvent utilization in the work-up procedure.

Conclusions

In this work, we demonstrated an unprecedented way of terpene biomass valorization to obtain phthalimides **4a–4s** under mechanochemical conditions. From solution-phase studies, we were able to demonstrate not only an improvement in the selectivity and yield of reactions but also to develop a more effective, faster, economical and safer protocol.

We developed a mild, scalable, and solvent-free protocol for synthesizing terpene-derived phthalimides, demonstrating mechanochemistry's utility in biomass valorization. The two-step one-pot milling protocol developed utilized cheap materials and implemented energy saving due to no heating conditions. These mild protocols in the integrated one-pot milling process also avoid bulk use of solvent, encompassing many of the green chemistry principles. The DA step provides adducts up to quantitative yields, showing great structural versatility and robustness. The aromatisation step – although more challenging – was successfully unlocked through the use of iodine and TMG, achieving phthalimide yields of up to 82%. We also evaluated two green metrics to highlight overall sustainability benefits that arise from our work. This study exemplifies how the strategic use of enabling technologies such as mechanochemistry can unlock sustainable, solvent-free routes to high value-added molecules from renewable feedstocks, paving the way for greener and more efficient synthetic practices.

Author contributions

Conceptualization, JABCR and JCP; Data curation, JABCR; Funding acquisition, JCP; Investigation, JABCR and RRM; Methodology, JABCR; Project administration, JABCR, RRM and JCP; Resources, JCP; Supervision, JCP; Visualization, JABCR, RRM and JCP; Writing – original draft, JABCR and RRM; Writing – review & editing, JABCR, RRM, DLB and JCP.

Conflicts of interest

There are no conflicts to declare.

Data availability

The data supporting this article have been included as part of the supplementary information (SI). Supplementary information: experimental procedures, characterization data and NMR spectra. See DOI: <https://doi.org/10.1039/d5su00509d>.

Acknowledgements

The authors gratefully acknowledge the financial support from the São Paulo Research Foundation – FAPESP (JABCR, 2023/08725-6 and 2024/18431-2; RRM, 2019/26450-9 and 2022/03872-8; JCP, 2021/06661-5), the Brazilian National Council for Scientific and Technological Development – CNPq (JCP, 308540/2021-2), and the Coordination for the Improvement of Higher Education Personnel – CAPES (RRM, Finance Code 001). We thank EMU-FAPESP 2022/11152-5 and LIRMN (RRID:SCR_027247), from CEMU-IQ-UNICAMP for technical support. We dedicate this article to Professor S. V. Ley, whose vision and mentorship have inspired generations of chemists, in celebration of his 80th birthday.

Notes and references

- J. H. Clark, *Green Chem.*, 1999, **1**, 1–8.
- P. Anastas and N. Eghbali, *Chem. Soc. Rev.*, 2009, **39**, 301–312.
- P. T. Anastas, L. G. Heine and T. C. Williamson, *Green Chemical Syntheses and Processes: Introduction*, in *Green Chemical Syntheses and Processes*, ed. P. T. Anastas, L. G. Heine and T. C. Williamson, American Chemical Society, Washington, DC, 2000, pp. 1–6, ISBN: 9780841218208.
- F. Gomollón-Bel, *CI*, 2023, **45**, 14–22.
- T. Friščić, C. Mottillo and H. M. Titi, *Angew. Chem.*, 2020, **132**, 1030–1041.
- J. L. Howard, Q. Cao and D. L. Browne, *Chem. Sci.*, 2018, **9**, 3080–3094.
- J. Andersen and J. Mack, *Green Chem.*, 2018, **20**, 1435–1443.
- G. W. Wang, *Chem. Soc. Rev.*, 2013, **42**, 7668–7700.
- Q. Cao, J. L. Howard, E. Wheatley and D. L. Browne, *Angew. Chem., Int. Ed.*, 2018, **57**, 11339–11343.
- K. Kondo, K. Kubota and H. Ito, *Nat. Synth.*, 2025, 1–10.
- S. L. James, C. J. Adams, C. Bolm, D. Braga, P. Collier, T. Friščić, F. Grepioni, K. D. M. Harris, G. Hyett, W. Jones, A. Krebs, J. Mack, L. Maini, A. G. Orpen, I. P. Parkin, W. C. Shearouse, J. W. Steed and D. C. Waddell, *Chem. Soc. Rev.*, 2011, **41**, 413–447.
- J. F. Reynes, F. Leon and F. García, *ACS Org. Inorg. Au*, 2024, **4**, 432–470.
- C. B. Lennox, T. H. Borchers, L. Gonnet, C. J. Barrett, S. G. Koenig, K. Nagapudi and T. Friščić, *Chem. Sci.*, 2023, **14**, 7475–7481.
- Q. Cao, J. L. Howard, D. E. Crawford, S. L. James and D. L. Browne, *Green Chem.*, 2018, **20**, 4443–4447.
- N. Fantozzi, J. N. Volle, A. Porcheddu, D. Virieux, F. García and E. Colacino, *Chem. Soc. Rev.*, 2023, **52**, 6680–6714.
- K. J. Ardila-Fierro and J. G. Hernández, *ChemSusChem*, 2021, **14**, 2145–2162.
- J. L. Howard, W. Nicholson, Y. Sagatov and D. L. Browne, *Beilstein J. Org. Chem.*, 2017, **13**, 1950–1956.
- M. Schnürch, N. Biedermann, N. Biedermann and M. Schnürch, *Chem.–Eur. J.*, 2025, e202500798.
- T. Szuppa, A. Stolle, B. Ondruschka and W. Hopfe, *Green Chem.*, 2010, **12**, 1288–1294.



- 20 C. E. Vickers, T. C. Williams, B. Peng and J. Cherry, *Curr. Opin. Chem. Biol.*, 2017, **40**, 47–56.
- 21 A. J. D. Silvestre and A. Gandini, *Monomers, Polymers and Composites from Renewable Resources*, 2008, pp. 17–38.
- 22 R. A. González-Hernández, N. A. Valdez-Cruz and M. A. Trujillo-Roldán, *Chem. Pap.*, 2024, **78**(5), 2783–2810.
- 23 S. G. Hillier and R. Lathe, *J. Endocrinol.*, 2019, **242**, R9–R22.
- 24 F. Wang and Z. Tong, *ChemistrySelect*, 2016, **1**, 5538–5541.
- 25 Y. Xiao, Q. Meng, X. Pan, C. Zhang, Z. Fu and C. Li, *Green Chem.*, 2020, **22**, 4341–4349.
- 26 D. I. Collias, A. M. Harris, V. Nagpal, I. W. Cottrell and M. W. Schultheis, *Ind. Biotechnol.*, 2014, **10**, 91–105.
- 27 J. D. Tibbetts, D. Russo, A. A. Lapkin and S. D. Bull, *ACS Sustain. Chem. Eng.*, 2021, **9**, 8642–8652.
- 28 F. Neațu, G. Culică, M. Florea, V. I. Parvulescu and F. Cavani, *ChemSusChem*, 2016, **9**, 3102–3112.
- 29 V. Domingo, C. Prieto, L. Silva, J. M. L. Rodilla, J. F. Quílez Del Moral and A. F. Barrero, *J. Nat. Prod.*, 2016, **79**, 831–837.
- 30 R. Galaverna, L. P. Fernandes, D. L. Browne and J. C. Pastre, *React. Chem. Eng.*, 2019, **4**, 362–367.
- 31 A. Yildirim, U. Atmaca, A. Keskin, M. Topal, M. Çelik, I. Gülçin and C. T. Supuran, *Bioorg. Med. Chem.*, 2015, **23**, 2598–2605.
- 32 M. Yin, R. H. Natelson, A. A. Campos, P. Kolar and W. L. Roberts, *Fuel*, 2013, **103**, 408–413.
- 33 H. C. Genuino, S. Thiyagarajan, J. C. van der Waal, E. de Jong, J. van Haveren, D. S. van Es, B. M. Weckhuysen and P. C. A. Bruijninx, *ChemSusChem*, 2017, **10**, 277–286.
- 34 B. G. Jadhav and S. D. Samant, *Russ. J. Org. Chem.*, 2014, **50**, 1301–1305.
- 35 A. Tan, B. Koc, E. Sahin, N. H. Kishali and Y. Kara, *Synthesis*, 2011, **7**, 1079–1084.

